—Original Article—

Suppression of mosaic mutation by co-delivery of CRISPR associated protein 9 and three-prime repair exonuclease 2 into porcine zygotes via electroporation

Shiro YAMASHITA[1, 2], Yuhei KOGASAKA[1], Yuuki HIRADATE[2], Kentaro TANEMURA[2] and Yutaka SENDAI[1]

[1]*Biological Sciences Section, Central Research Institute for Feed and Livestock of Zen-noh, Ibaraki 300-4204, Japan*
[2]*Laboratory of Animal Reproduction and Development, Graduate School of Agricultural Science, Tohoku University, Miyagi 980-8572, Japan*

Abstract. Gene-modified animals, including pigs, can be generated efficiently by introducing CRISPR associated protein 9 (CRISPR/Cas9) into zygotes. However, in many cases, these zygotes tend to become mosaic mutants with various different mutant cell types, making it difficult to analyze the phenotype of gene-modified founder animals. To reduce the mosaic mutations, we introduced three-prime repair exonuclease 2 (Trex2), an exonuclease that improves gene editing efficiency, into porcine zygotes along with CRISPR/Cas9 via electroporation. Although the rate of porcine blastocyst formation decreased due to electroporation ($25.9 \pm 4.6\%$ *vs*. $41.2 \pm 2.0\%$), co-delivery of murine Trex2 (mTrex2) mRNA with CRISPR/Cas9 did not affect it any further ($25.9 \pm 4.6\%$ *vs*. $31.0 \pm 4.6\%$). In addition, there was no significant difference in the diameter of blastocysts carrying CRISPR/Cas9 (164.7 ± 10.2 μm), and those with CRISPR/Cas9 + mTrex2 (151.9 ± 5.1 μm) as compared to those from the control group (178.9 ± 9.0 μm). These results revealed that mTrex2 did not affect the development of pre-implantation embryo. We also found bi-allelic, as well as mono-allelic, non-mosaic homozygous mutations in the blastocysts. Most importantly, co-delivery of mTrex2 mRNA with CRISPR/Cas9 increased non-mosaic mutant blastocysts ($29.3 \pm 4.5\%$) and reduced mosaic mutant blastocysts ($70.7 \pm 4.5\%$) as compared to CRISPR/Cas9 alone ($5.6 \pm 6.4\%$ and $92.6 \pm 8.6\%$, respectively). These data suggest that the co-delivery of CRISPR/Cas9 and mTrex2 is a useful method to suppress mosaic mutation.

Key words: CRISPR associated protein 9 (CRISPR/Cas9), Electroporation, Gene editing, Mosaic mutants, Three-prime repair exonuclease 2 (Trex2) exonuclease

Pig is now regarded as a useful model to study human health and disease because of its similarity to humans in terms of size, physiology, and genetics [1, 2]. Various gene-modified pig models such as for cancer [3], hyperlipidemia [4, 5], immunodeficiency [6], and muscular dystrophy [7] have been generated to study these human diseases. In addition, an α-1,3-galactosyltransferase knockout line for studying xenotransplantation has been established [8]. These gene-modified pig lines are generated by somatic cell nuclear transfer (SCNT) from gene-modified primary fibroblast cells. However, SCNT is a difficult technique with very low efficiency.

In recent years, gene editing tools, such as zinc finger nuclease (ZFN) [9], transcription activator-like effector nuclease (TALEN) [10], and clustered regularly interspaced short palindromic repeats/ CRISPR associated protein 9 (CRISPR/Cas9) [11, 12] have been developed. These nucleases induce site-specific double-strand breaks

in DNA, and while repairing these through non-homologous end joining (NHEJ), desired nucleotide sequences can be edited, causing mutations. Various animal models can be generated easily by introducing these tools into zygotes via microinjection [13–16] or more recently adapted method of electroporation. The latter includes the technique for animal knockout system by electroporation (TAKE) [17, 18] and gene editing by electroporation (GEEP) of Cas9 protein [19], for generating gene-modified rodents [17, 18, 20] and pigs [19]. However, sometimes DNA editing is not completed before DNA replication in one-cell-stage zygotes, and the wild-type (WT) alleles remain unchanged. After early embryonic cleavage, NHEJ repair pathway error induces random indel mutation at each of the further cleavages. This is one of the reasons why gene editing in zygotes tends to produce mosaicism [21–23]. Therefore, in many cases, it is difficult to obtain the founder animals with uniform phenotype that allows phenotypic analysis; instead, their progenies are needed to be studied to avoid the effects of mosaic mutations. However, this may take considerable time, especially for larger animals, including pigs. In mice, the problem of mosaic mutations can be overcome to some degree by introducing Cas9 protein into early-stage zygotes [24]. However, it is still a major issue in larger animals such as pigs [15, 19, 25], cattle [26], and nonhuman primates [16]. These embryos, developed using gene editing tools, tend to exhibit a high level of

mosaicism [22]. Various efforts have been made to reduce mosaic mutations. These include tagging Cas9 with ubiquitin–proteasomal degradation signals to limit their active period in nonhuman primates [27], introducing CRISPR/Cas9 at the most appropriate time in porcine zygotes [28], and introducing multiple single-guide RNAs (sgRNAs) into zygotes to make phenotypically non-mosaic homozygous mutant animals, despite their genetic mosaicism [29]. However, this issue has not been resolved yet.

Ideally, mutations should be induced in one-cell-stage zygotes before DNA replication to avoid mosaicism. It is important that not only the DNA is cleaved by CRISPR/Cas9, but also the repair of DNA errors occurs before DNA replication in one-cell-stage zygotes [23]. It has been reported that the introduction of TALEN with exonuclease I into rat zygotes enhanced the efficiency of gene editing [14]. Among the different exonucleases that were co-delivered with a homing endonuclease, ZFN or TALEN into HEK293 cells, murine three-prime repair exonuclease 2 (mTrex2) was found to be the one to improve the efficiency of gene editing to the greatest extent [30]. Trex2 is involved in maintenance of replication forks [31] and the DNA repair pathway through its 3′ to 5′ exonuclease activity [32].

Exonucleases are thought to improve gene editing efficiency by digesting DNA ends that are excised by gene editing tools. Therefore, we hypothesized that the co-delivery of CRISPR/Cas9 and mTrex2 may enhance mutation induction at an early stage, while reducing mosaic mutations. We introduced Cas9 protein, sgRNA, and mTrex2 mRNA into porcine zygotes via electroporation, and analyzed the mutation rates and mosaic mutations, using Tracking of Indels by Decomposition (TIDE) software [33].

Materials and Methods

In vitro transcription of murine Trex2 mRNA and sgRNA

Total RNA was extracted from mouse embryonic fibroblast (MEF) feeder cells (Cell Biolabs, San Diego, CA, USA) using ISOGEN (Nippon Gene, Toyama, Japan), following the manufacturer's protocol, and reverse transcribed using Oligo dT primer and ReverTraAceα Kit (Toyobo, Tokyo, Japan). mTrex2 cDNA was amplified using PrimeSTAR-GXL DNA polymerase (Takara, Kusatsu, Japan) and the primer set: Trex2 mouse 52(T) (5′-aggcctcattgttcctgtga-3′) and Trex2 mouse 964(B) (5′-agccctgaaagagcaactca-3′). PCR was performed by initial incubation at 95°C for 3 min; followed by 35 cycles of 98°C for 10 sec, 57°C for 15 sec, and 68°C for 40 sec; and finally, 68°C for 8 min. Resultant PCR products were subcloned into pCR-BluntII vector (Thermo Fisher Scientific, Waltham, MA, USA) and cloned into pcDNA3.1(+) vector (Thermo Fisher Scientific), using *Eco*RI. Polyadenylation signal sequence and terminator sequence were attached to the 3′ end of the mTrex2 cDNA (Supplementary Fig. 1: online only). These sequences were synthesized by Thermo Fisher Scientific using pXT7 hCas9 plasmid sequence [34] as a reference. This vector was linearized using *Xba*I and mTrex2 mRNA was transcribed using mMESSAGE mMACHINE T7 Kit (Thermo Fisher Scientific). sgRNA targeting the *GHR* gene was designed using a CRISPR design tool [35]. The PCR was performed using Phusion High-Fidelity Master Mix (New England BioLabs, Beverly, MA, USA) and pD1401 vector (ATUM, Newark, CA, USA) as a template, using the following primer set: T7-GHR-gRNA27-scaffold28(T)

(5′-TAATACGACTCACTATAGACTGGGCTGCTGGGTAGC-AGGTTTTAGAGCTAGAAATAGCAAGTTAAA-3′) and gRNA scaffold T1 Ver(B) (5′-AGCACCGACTCGGTGCCACT-3′). The PCR was performed by initial incubation at 95°C for 3 min, followed by 45 cycles of 98°C for 10 sec and 68°C for 40 sec, and finally 68°C for 8 min. The PCR product was purified using QIAquick PCR Purification Kit (QIAGEN, Hilden, Germany) and sgRNA was transcribed using MEGAshortscript T7 Kit (Thermo Fisher Scientific). These RNAs were purified by phenol/chloroform extraction and dissolved into Opti-MEM medium (Thermo Fisher Scientific). Concentration of these RNAs was measured using a Qubit 2.0 Fluorometer (Thermo Fisher Scientific) and Qubit RNA BR Assay Kit (Thermo Fisher Scientific).

Oocyte collection

Porcine ovaries were collected from 5–6-month-old crossbred gilts (Landrace × Large White × Duroc) which were produced for meat production at the slaughterhouse of our laboratory. Cumulus oocyte complexes (COCs) were collected by cutting vesicular follicles in POE-CM medium (Research Institute for Functional Peptides, Yamagata, Japan) and washed several times.

In vitro maturation (IVM)

COCs with two to three layers of cumulus cells were cultured in maturation medium at 39°C in a humidified incubator containing 5% CO_2 and 5% O_2. Maturation medium was made by adding 1 mM dibutyryl cyclic AMP (dbcAMP; Research Institute for Functional Peptides), 0.5 U/ml recombinant human follicle stimulating hormone (rFSH, GONAL-f; Merck Serono, Coinsins, Switzerland) and 10 ng/ml transforming growth factor-α (TGF-α; Research Institute for Functional Peptides) to POM medium (Research Institute for Functional Peptides). After 22 h of incubation, COCs were moved to maturation medium without dbcAMP and rFSH for 24 h.

In vitro fertilization (IVF)

Duroc semen for IVF was purchased from Zen-noh Livestock (Tokyo, Japan) and stored at 17°C until IVF. Ten milliliters of semen was centrifuged at 700 g for 10 min and the pelleted spermatozoa was resuspended in 400 μl of SEM-5x (Research Institute for Functional Peptides), out of which, 200 μl of it was mixed with 1 ml of 50% Percoll. It was layered on 80% Percoll in a 15-ml conical tube and centrifuged at 700 *g* for 20 min. The spermatozoon pellet was then resuspended in PFM medium (Research Institute for Functional Peptides) to get a count of $1.0 × 10^6$ cells/ml. Matured COCs were transferred to PFM medium containing spermatozoa and co-cultured for 20 h.

Electroporation and in vitro culture (IVC)

Electroporation of CRISPR/Cas9 and mTrex2 mRNA into porcine zygotes was performed using NEPA21 Super Electroporator (NEPAGENE, Ichikawa, Japan) and CUY520P5 electrode (NEPAGENE). Recombinant Sp Cas9 (Alt-R S.P. Cas9 Nuclease; Integrated DNA Technologies, Coralville, IA, USA) (200 ng/μl), sgRNA (200 ng/μl), and mTrex2 mRNA (500 ng/μl) were dissolved in 40 μl of Opti-MEM medium and put into the electrode. After IVF, COCs were transferred to 1 ml of POE-CM medium and had their cumulus cells removed by vortexing. Inseminated zygotes were

washed several times in Opti-MEM medium and transferred into the electrode. A total of 20–30 porcine inseminated zygotes were used for each electroporation procedure. Electroporation was performed using a poring pulse (voltage: 225 V, pulse width: 2.5 msec, pulse interval: 50 msec, decay rate: 10%, number of pulses: 4) and a transfer pulse (voltage: 20 V, pulse width: 50 msec, pulse interval: 50 msec, decay rate: 40%, number of pulses: ± 5). The electroporation condition and the concentration of mTrex2 mRNA were optimized using GFP mRNA beforehand. The concentration of Cas9 protein and sgRNA were optimized using previously reported data [18] as a reference. After electroporation, zygotes were transferred into PZM-5 medium (Research Institute for Functional Peptides) and cultured at 39°C in a humidified incubator containing 5% CO_2 and 5% O_2. After 4 days, embryos were transferred into PBM medium (Research Institute for Functional Peptides) and cultured for 2 days. As a control, some inseminated zygotes were cultured under the same conditions but without electroporation. The rate of zygotes developed to blastocysts was calculated on day 6 after IVF.

Morphological analysis of porcine blastocysts

Porcine blastocysts were imaged on day 6 after IVF, using an inverted microscope (IX71; Olympus, Tokyo, Japan), a digital camera (DP71; Olympus), and cellSens Standard software. The diameter of blastocysts was measured by image analysis using the software.

PCR amplification for blastocyst-stage embryos

Genomic DNA of blastocyst-stage embryos was extracted using 10 µl of 25 mM NaOH + 200 µM EDTA by heating at 95°C for 10 min. The CRISPR/Cas9 target region was amplified using Terra PCR Direct Polymerase (Takara) and primer set: GHR exon 9 Surveyor (T) (5′-gctcgatattgatgaccctg-3′) and GHR 159(T) (5′-ttggagcacattct-gctgtc-3′). PCR was performed with initial incubation at 95°C for 3 min; followed by 35 cycles of 98°C for 10 sec, 57°C for 15 sec, and 68°C for 40 sec; and finally 68°C for 8 min.

Analysis of mutation and mosaicism (genotyping)

PCR products containing the CRISPR/Cas9 target region were purified using QIAquick PCR Purification Kit (Qiagen) and sequenced by Sanger's method using GHR exon 9 Surveyor(T) primer (5′-gctc-gatattgatgaccctg-3′) and ABI 3130 sequencer (Applied Biosystems, Foster City, CA, USA), in accordance with the manufacturer's protocol. Small indels were analyzed using TIDE software. The indel size range was set to maximize the R^2 value for each embryo. Blastocysts with more than three alleles or two different alleles at rates of more than 25% were judged as exhibiting mosaicism. Blastocysts with low R^2 values of less than 0.9 were subjected to electrophoresis using an MCE-202 MultiNA microchip electrophoresis system (Shimazu, Kyoto, Japan) and DNA-1000 Kit (Shimazu) to identify large indels of more than 50 bp. Mosaic mutations were scored by counting the number of bands.

Statistical analysis

The blastocyst development rate and diameter of blastocysts were analyzed by the Tukey-Kramer test. The percentage of mutations and mosaic mutation rates were calculated using *t*-test. P < 0.05 was considered statistically significant.

Results

Effect of electroporation procedure and Trex2 introduction on blastocyst development

To measure the effect of introducing CRISPR/Cas9 and mTrex2 mRNA by electroporation on blastocyst development, the blastocyst production rate and their morphology were compared on day 6 after IVF. Although the production rate of porcine blastocysts (41.2 ± 2.0%) decreased by the electroporation procedure (25.9 ± 4.6%), co-delivery of mTrex2 mRNA with CRISPR/Cas9 did not change it (31.0 ± 4.6%) significantly. In addition, there was no difference in the diameters of blastocysts because of CRISPR/Cas9 (164.7 ± 10.2 µm), or CRISPR/Cas9 + Trex2 (151.9 ± 5.1 µm) as compared to those of the control group (178.9 ± 9.0 µm) at day 6 after IVF (Fig. 2, Table 2).

*Rate of mutations introduced by CRISPR/Cas9*

Analysis of CRISPR/Cas9 targeting region showed that on day 6 after IVF, introduction of CRISPR/Cas9 alone created about 64% of blastocysts with complete gene modification carrying no WT alleles and about 31% with partial modification carrying WT alleles, while inclusion of mTrex2 did not alter these proportion significantly (approximately 79% and 21%, respectively) (Fig. 1B and C, Table 1).

Mosaic mutation rate

Analyses of mutations and mosaic mutations revealed numerous mosaic blastocysts with more than three alleles (Fig. 3A) or the presence of two different alleles at rates of more than 25% (Fig. 3B). TIDE software cannot estimate indels larger than 50 bp, so the R^2 value becomes low, when larger than 50 bp indels are introduced (Fig. 3C). To overcome this, blastocysts with R^2 values less than 0.9, were analyzed by electrophoresing the PCR products and their mosaicism was determined using the number of bands (Fig. 3D). The results showed that all blastocysts with an R^2 value less than 0.9, were mosaics. Introducing CRISPR/Cas9 by electroporation resulted in production of non-mosaic homozygous mutant blastocysts with both two different alleles (Fig. 4A) as well as with the same alleles (Fig. 4B). Co-delivery of mTrex2 mRNA with CRISPR/Cas9 increased the production of non-mosaic mutant blastocysts (29.3 ± 4.5), and reduced the mosaic mutant blastocysts (70.7 ± 4.5%) compared with CRISPR/Cas9 alone (5.6 ± 6.4% and 92.6 ± 8.6%, respectively) (Table 1). To determine the genotype of non-mosaic homozygous mutant blastocysts, their PCR products were subcloned into a plasmid vector and sequenced. The results revealed that they had the same indel size as estimated by TIDE software (Fig. 4C). The number of alleles could not be determined for blastocysts with indels larger than 50 bp, but TIDE software detected a few blastocysts with as many as seven alleles (Fig. 3A).

Discussion

Recently, gene-modified pigs are being used to study human diseases as they have become easier to generate through gene editing tools inserted into zygotes through microinjection or electroporation [15, 19, 25]. However, these procedures result in mosaic mutations in the resultant gene-modified animals [15, 19, 25]. To avoid these,
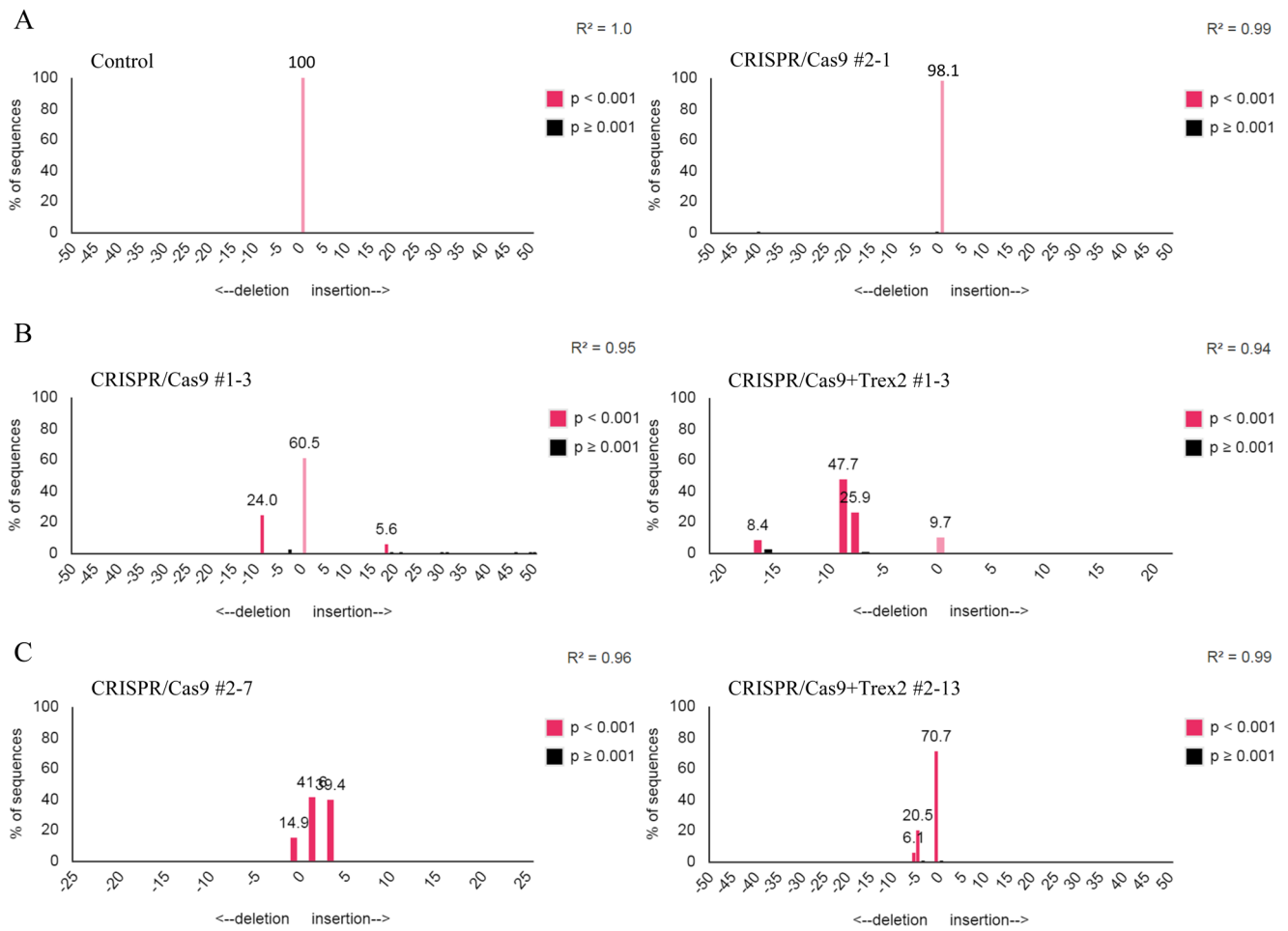
Fig. 1. Analysis of gene modification conditions using TIDE software. The bar in deep pink indicates mutant allele, that in light pink indicates wild-type allele, and that in black indicates noise. A. Wild-type blastocysts. B. Partially gene-modified blastocysts carrying wild-type allele. C. Completely gene-modified blastocysts with no wild-type allele.
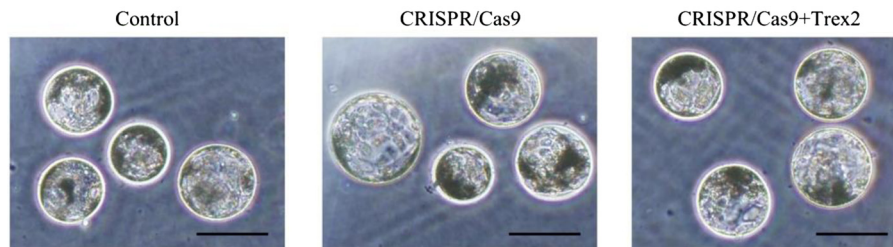
Fig. 2. Comparison of blastocyst morphology on day 6 after *in vitro* fertilization (IVF). Each scale bar indicates 200 µm.

mutations need to be introduced in one-cell-stage zygotes before DNA replication. We hypothesized that the co-delivery of mTrex2 with CRISPR/Cas9 may promote early induction of mutations, leading to reduction of mosaicism. We introduced Cas9 protein, sgRNA, and mTrex2 mRNA into porcine zygotes through electroporation.

It was reported in mouse zygotes that electroporation of CRISPR/ Cas9 was less effective for embryogenesis than microinjection [17, 18]; and that the electroporation procedure did not affect the blastocyst production rate in porcine zygotes [19]. In the present study too, co-delivery of CRISPR/Cas9 with mTrex2 mRNA did not affect the blastocyst production rate, but the electroporation procedure per se had an effect, when compared with the control

Table 1. Rates of blastocyst production and gene modification

	Cas9 protein (ng/μl)	sgRNA (ng/μl)	mTrex2 mRNA (ng/μl)	No. of total zygotes	Zygotes developed to blastocysts (%)	Wild type blastocysts (%)	Partially modified blastocysts (%)	Completely modified blastocysts (%)	Mosaic blastocysts (%)	Non-mosaic blastocysts (%)
Control	-	-	-	144	60 (41.2 ± 2.0) [a]	-	-	-		
CRISPR/Cas9	200	200	0	144	38 (25.9 ± 4.6) [b]	1 (4.8 ± 5.5)	12 (30.8 ± 17.7)	25 (64.4 ± 15.5)	34 (92.6 ± 8.6) [a]	3 (5.6 ± 6.4) [a]
CRISPR/Cas9+Trex2	200	200	500	143	45 (31.0 ± 2.6) [ab]	0 (0.0 ± 0.0)	10 (21.2 ± 7.8)	35 (78.8 ± 7.8)	32 (70.7 ± 4.5) [b]	13 (29.3 ± 4.5) [b]

Three replicate trials were carried out. Percentages are expressed as the mean ± SEM. The Tukey Kramer test showed significant differences in the blastocyst production rate between values with different lower-case letters. The *t*-test showed a significant difference in production rates of the mosaic and non-mosaic blastocyst between values with different lower-case letters (P < 0.05).

Table 2. Comparison of blastocyst diameter on day 6 after *in vitro* fertilization (IVF)

	No. of blastocyst	Diameter of blastocyst (μm)
Control	27	178.9 ± 9.0
CRISPR/Cas9	18	164.7 ± 10.2
CRISPR/Cas9 + Trex2	21	151.9 ± 5.1

Diameters of blastocysts are expressed as the mean ± SEM.

group (Table 1). Diameter of blastocysts also showed no difference on day 6 after IVF (Table 2). Present study showed that co-delivery of CRISPR/Cas9 with mTrex2 mRNA did not affect the development of pre-implantation embryo. However, it is necessary to study the effects of the electroporation on offspring before generalizing this observation. Against this background, although more detailed study of the electroporation conditions is needed, it appears that the co-delivery of CRISPR/Cas9 and mTrex2 mRNA is a useful method to generate gene-edited pigs. Some mosaic blastocysts with up to seven alleles were observed by TIDE software analysis (Fig. 3A), which means that the introduction of mutation by CRISPR/Cas9 continues to occur at least until the embryos reach four-cell stage. In case of mice, a few embryos and pups were reported to show five alleles, but most of them had four or fewer alleles, when Cas9 protein and sgRNA were introduced into zygotes [24, 36]. This suggests that mutations are introduced by CRISPR/Cas9 until the two-cell stage in mouse embryos. Consequently, it appears that retention of CRISPR/Cas9 activity is for longer duration in porcine embryos than in murine ones, because of which porcine embryos show a greater tendency for high mosaicism.

As CRISPR/Cas9 introduces mutations until the embryo reaches at least four-cell stage, we considered that, when two different alleles were identified by TIDE software in the mosaic embryos, the difference of their composition becomes 25% at minimum, because there were 5 same-sequence alleles (62.5%) out of 8, and another 3 same-sequence alleles (37.5%), at four-cell stage. Therefore, embryos with two different alleles at rates of more than 25% or with more than three alleles, were considered as mosaics. Embryos were classified as non-mosaics, if they carry two different alleles at rates of less than 25% or have only one allele of the same sequence.

In this study, we succeeded in reducing mosaic mutation by co-delivery of CRISPR/Cas9 and mTrex2 mRNA. It appears that mutations are introduced rapidly by CRISPR/Cas9, inducing a double-strand break and simultaneously, mTrex2 digesting the newly formed DNA-ends in one-cell-stage zygotes before DNA replication. Various efforts have been made to suppress mosaic mutations, such as introducing CRISPR/Cas9 into early-stage zygotes [24] and tagging Cas9 with ubiquitin-proteasomal degradation signals to limit its active period [27]. Present study is the first to reduce mosaic mutations by the co-delivery of exonuclease and CRISPR/Cas9. However, it was reported that the co-delivery of Trex2 and CRISPR/Cas9 introduced larger deletions [37, 38]. It is possible that a large-scale deletion occurred in our study as well, but could not be detected using PCR amplification of the 650 bp target sequence and TIDE software. To resolve this, it is necessary to detect all mutation by whole-genome sequencing or the combination of large-scale PCR and long-read nanopore sequencing [39]. It appears that mosaicism was reduced because of mTrex2 inducing DNA digestion after cleavage by CRISPR/Cas9 at an early stage, but it is still unclear when does the mTrex2 mRNA is translated into a protein, when does the CRISPR/Cas9 introduce mutation, and how useful this approach is for other genetic loci. To answer these questions, detailed analysis needs to be carried out.

Some non-mosaic homologous mutant embryos with in-frame mutations were identified in this study (Fig. 4D). Mutations that are introduced by CRISPR/Cas9 and NHEJ pathway are random, and therefore, co-delivery of single-stranded oligo DNA (ssODN) for knock-in (KI), along with CRISPR/Cas9 may help in efficiently create out-of-frame mutants. However, the efficiency of KI by the co-delivery of ssODN is reported to be lower than that of NHEJ pathway mutation [40, 41]. Imprecise mutations often occur and embryos with these tend to exhibit mosaicism with WT, NHEJ, and KI alleles [40, 41]. Moreover, Trex2 is known to inhibit homologous recombination [38], and therefore, it will be difficult to overcome this problem by introducing the combination of Trex2 and ssODN. It is also necessary to develop an alternate method to introduce out-of-frame mutation efficiently. In any case, present study suggests that significant number of non-mosaic homozygous mutant pigs can be generated by the co-delivery of CRISPR/Cas9 and mTrex2 without highly technical manipulation, such as microinjection and SCNT. However, using this method we could not suppress mosaic mutations completely. Therefore, other approaches such as using exonucleases that have higher activity in porcine embryos and using a system that accumulates Trex2 at double-strand break sites [42] may reduce mosaic mutations further.
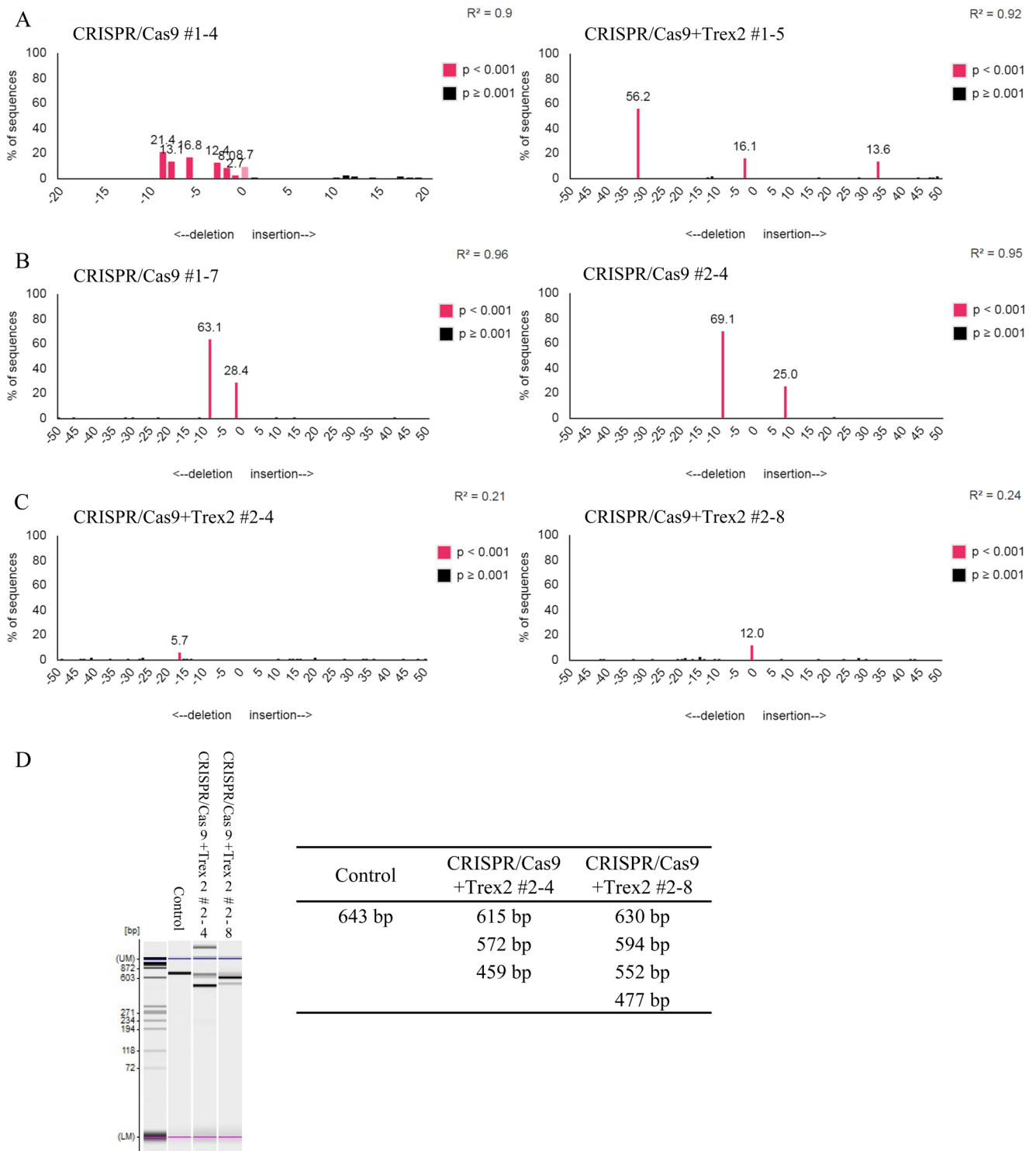
Fig. 3. Analysis of mosaic mutant blastocysts using TIDE software and electrophoresis. Bar in deep pink indicates mutant allele, that in light pink indicates wild-type allele, and the black one indicates noise. A: Blastocysts with more than three alleles. B: Blastocysts with two different alleles at rates of more than 25%. C: Blastocysts with R² < 0.9 because of indels larger than 50 bp. D: Electrophoretic analysis of blastocysts with indels larger than 50 bp.
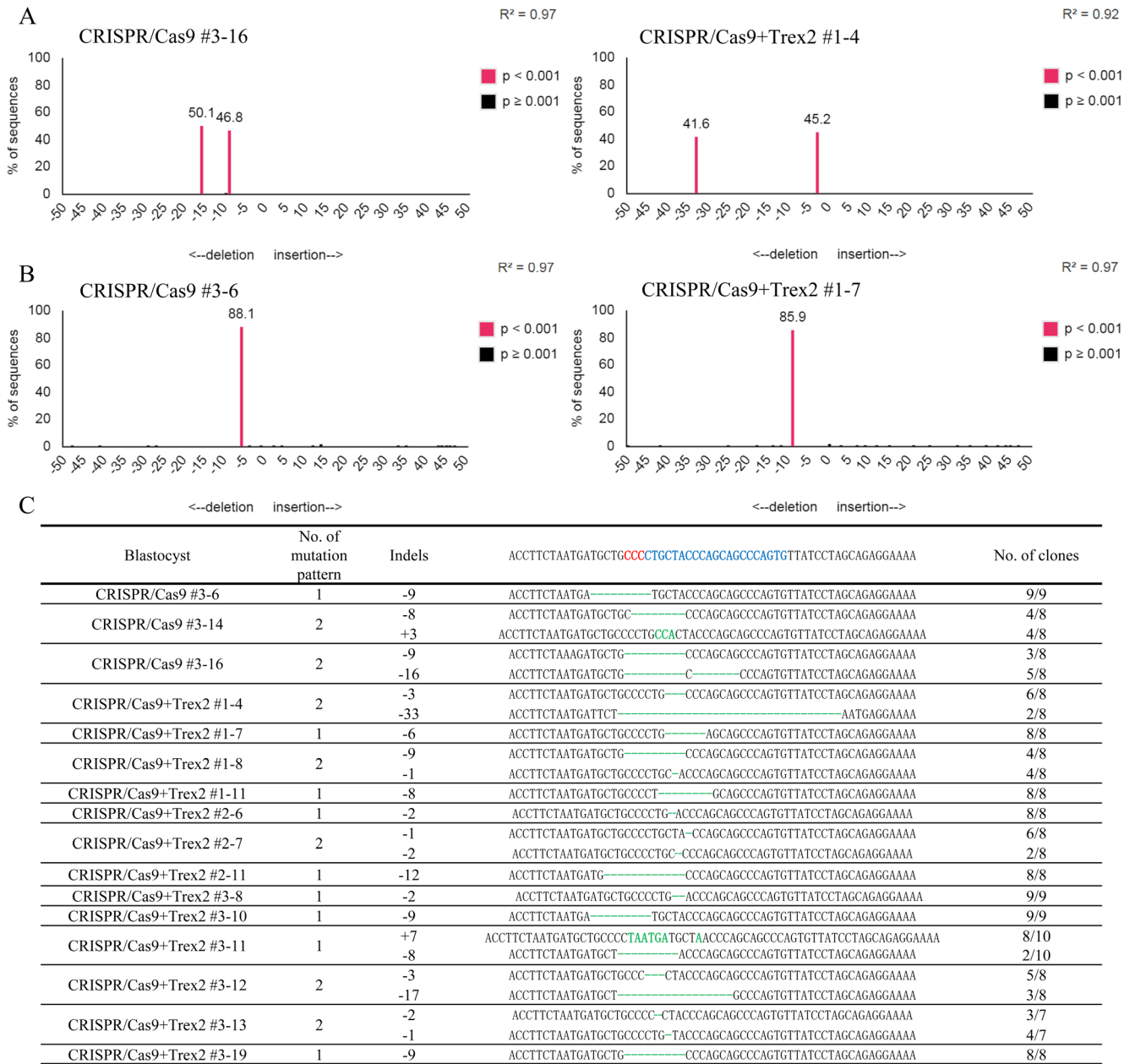
Fig. 4. Analysis of non-mosaic homozygous mutant blastocysts using TIDE software. The bar in deep pink indicates mutation allele and that in black indicates noise. A: Non-mosaic homozygous mutant blastocysts with two different mutation alleles. B: Non-mosaic homozygous mutant blastocysts carrying alleles with the same sequence mutation. C: CRISPR/Cas9 targeting sequence and mutant sequence of non-mosaic homozygous mutant blastocysts. Nucleotides in blue show the target sequence, those in red indicate the PAM sequence, and those in green are indel mutations.

Acknowledgments

References

1. **Walters EM, Prather RS.** Advancing swine models for human health and diseases. *Mo Med* 2013; **110**: 212–215. [Medline]
2. **Whyte JJ, Prather RS.** Genetic modifications of pigs for medicine and agriculture. *Mol Reprod Dev* 2011; **78**: 879–891. [Medline] [CrossRef]
3. **Sieren JC, Meyerholz DK, Wang X-J, Davis BT, Newell JD Jr, Hammond E, Rohret JA, Rohret FA, Struzynski JT, Goeken JA, Naumann PW, Leidinger MR, Taghiyev A, Van Rheeden R, Hagen J, Darbro BW, Quelle DE, Rogers CS.** Development and

translational imaging of a TP53 porcine tumorigenesis model. *J Clin Invest* 2014; **124**: 4052–4066. [Medline] [CrossRef]

4. **Li Y, Fuchimoto D, Sudo M, Haruta H, Lin Q-F, Takayama T, Morita S, Nochi T, Suzuki S, Sembon S, Nakai M, Kojima M, Iwamoto M, Hashimoto M, Yoda S, Kunimoto S, Hiro T, Matsumoto T, Mitsumata M, Sugitani M, Saito S, Hirayama A, Onishi A.** Development of human-like advanced coronary plaques in low-density lipoprotein receptor knockout pigs and justification for statin treatment before formation of atherosclerotic plaques. *J Am Heart Assoc* 2016; **5**: e002779. [Medline] [CrossRef]

5. **Davis BT, Wang X-J, Rohret JA, Struzynski JT, Merricks EP, Bellinger DA, Rohret FA, Nichols TC, Rogers CS.** Targeted disruption of LDLR causes hypercholesterolemia and atherosclerosis in Yucatan miniature pigs. *PLoS One* 2014; **9**: e93457. [Medline] [CrossRef]

6. **Ito T, Sendai Y, Yamazaki S, Seki-Soma M, Hirose K, Watanabe M, Fukawa K, Nakauchi H.** Generation of recombination activating gene-1-deficient neonatal piglets: a model of T and B cell deficient severe combined immune deficiency. *PLoS One* 2014; **9**: e113833. [Medline] [CrossRef]

7. **Klymiuk N, Blutke A, Graf A, Krause S, Burkhardt K, Wuensch A, Krebs S, Kessler B, Zakhartchenko V, Kurome M, Kemter E, Nagashima H, Schoser B, Herbach N, Blum H, Wanke R, Aartsma-Rus A, Thirion C, Lochmüller H, Walter MC, Wolf E.** Dystrophin-deficient pigs provide new insights into the hierarchy of physiological derangements of dystrophic muscle. *Hum Mol Genet* 2013; **22**: 4368–4382. [Medline] [CrossRef]

8. **Phelps CJ, Koike C, Vaught TD, Boone J, Wells KD, Chen S-H, Ball S, Specht SM, Polejaeva IA, Monahan JA, Jobst PM, Sharma SB, Lamborn AE, Garst AS, Moore M, Demetris AJ, Rudert WA, Bottino R, Bertera S, Trucco M, Starzl TE, Dai Y, Ayares DL.** Production of alpha 1,3-galactosyltransferase-deficient pigs. *Science* 2003; **299**: 411–414. [Medline] [CrossRef]

9. **Kim YG, Cha J, Chandrasegaran S.** Hybrid restriction enzymes: zinc finger fusions to Fok I cleavage domain. *Proc Natl Acad Sci USA* 1996; **93**: 1156–1160. [Medline] [CrossRef]

10. **Christian M, Cermak T, Doyle EL, Schmidt C, Zhang F, Hummel A, Bogdanove AJ, Voytas DF.** Targeting DNA double-strand breaks with TAL effector nucleases. *Genetics* 2010; **186**: 757–761. [Medline] [CrossRef]

11. **Jinek M, Chylinski K, Fonfara I, Hauer M, Doudna JA, Charpentier E.** A programmable dual-RNA-guided DNA endonuclease in adaptive bacterial immunity. *Science* 2012; **337**: 816–821. [Medline] [CrossRef]

12. **Cong L, Ran FA, Cox D, Lin S, Barretto R, Habib N, Hsu PD, Wu X, Jiang W, Marraffini LA, Zhang F.** Multiplex genome engineering using CRISPR/Cas systems. *Science* 2013; **339**: 819–823. [Medline] [CrossRef]

13. **Wang H, Yang H, Shivalila CS, Dawlaty MM, Cheng AW, Zhang F, Jaenisch R.** One-step generation of mice carrying mutations in multiple genes by CRISPR/Cas-mediated genome engineering. *Cell* 2013; **153**: 910–918. [Medline] [CrossRef]

14. **Mashimo T, Kaneko T, Sakuma T, Kobayashi J, Kunihiro Y, Voigt B, Yamamoto T, Serikawa T.** Efficient gene targeting by TAL effector nucleases coinjected with exonucleases in zygotes. *Sci Rep* 2013; **3**: 1253. [Medline] [CrossRef]

15. **Wang Y, Du Y, Shen B, Zhou X, Li J, Liu Y, Wang J, Zhou J, Hu B, Kang N, Gao J, Yu L, Huang X, Wei H.** Efficient generation of gene-modified pigs via injection of zygote with Cas9/sgRNA. *Sci Rep* 2015; **5**: 8256. [Medline] [CrossRef]

16. **Chen Y, Zheng Y, Kang Y, Yang W, Niu Y, Guo X, Tu Z, Si C, Wang H, Xing R, Pu X, Yang SH, Li S, Ji W, Li XJ.** Functional disruption of the dystrophin gene in rhesus monkey using CRISPR/Cas9. *Hum Mol Genet* 2015; **24**: 3764–3774. [Medline] [CrossRef]

17. **Kaneko T, Sakuma T, Yamamoto T, Mashimo T.** Simple knockout by electroporation of engineered endonucleases into intact rat embryos. *Sci Rep* 2014; **4**: 6382. [Medline] [CrossRef]

18. **Kaneko T, Mashimo T.** Simple genome editing of rodent intact embryos by electroporation. *PLoS One* 2015; **10**: e0142755. [Medline] [CrossRef]

19. **Tanihara F, Takemoto T, Kitagawa E, Rao S, Do LTK, Onishi A, Yamashita Y, Kosugi C, Suzuki H, Sembon S, Suzuki S, Nakai M, Hashimoto M, Yasue A, Matsuhisa M, Noji S, Fujimura T, Fuchimoto D, Otoi T.** Somatic cell reprogramming-free generation of genetically modified pigs. *Sci Adv* 2016; **2**: e1600803. [Medline] [CrossRef]

20. **Hashimoto M, Takemoto T.** Electroporation enables the efficient mRNA delivery into the mouse zygotes and facilitates CRISPR/Cas9-based genome editing. *Sci Rep* 2015; **5**: 11315. [Medline] [CrossRef]

21. **Mehravar M, Shirazi A, Nazari M, Banan M.** Mosaicism in CRISPR/Cas9-mediated genome editing. *Dev Biol* 2019; **445**: 156–162. [Medline] [CrossRef]

22. **Lamas-Toranzo I, Ramos-Ibeas P, Pericuesta E, Bermejo-Álvarez P.** Directions and applications of CRISPR technology in livestock research. *Anim Reprod* 2018; **15**: 292–300. [CrossRef]

23. **Hsu PD, Lander ES, Zhang F.** Development and applications of CRISPR-Cas9 for genome engineering. *Cell* 2014; **157**: 1262–1278. [Medline] [CrossRef]

24. **Hashimoto M, Yamashita Y, Takemoto T.** Electroporation of Cas9 protein/sgRNA into early pronuclear zygotes generates non-mosaic mutants in the mouse. *Dev Biol* 2016; **418**: 1–9. [Medline] [CrossRef]

25. **Sato M, Koriyama M, Watanabe S, Ohtsuka M, Sakurai T, Inada E, Saitoh I, Nakamura S, Miyoshi K.** Direct injection of CRISPR/Cas9-related mRNA into cytoplasm of parthenogenetically activated porcine oocytes causes frequent mosaicism for indel mutations. *Int J Mol Sci* 2015; **16**: 17838–17856. [Medline] [CrossRef]

26. **Bevacqua RJ, Fernandez-Martín R, Savy V, Canel NG, Gismondi MI, Kues WA, Carlson DF, Fahrenkrug SC, Niemann H, Taboga OA, Ferraris S, Salamone DF.** Efficient edition of the bovine PRNP prion gene in somatic cells and IVF embryos using the CRISPR/Cas9 system. *Theriogenology* 2016; **86**: 1886–1896.e1. [Medline] [CrossRef]

27. **Tu Z, Yang W, Yan S, Yin A, Gao J, Liu X, Zheng Y, Zheng J, Li Z, Yang S, Li S, Guo X, Li XJ.** Promoting Cas9 degradation reduces mosaic mutations in non-human primate embryos. *Sci Rep* 2017; **7**: 42081. [Medline] [CrossRef]

28. **Sato M, Kosuke M, Koriyama M, Inada E, Saitoh I, Ohtsuka M, Nakamura S, Sakurai T, Watanabe S, Miyoshi K.** Timing of CRISPR/Cas9-related mRNA microinjection after activation as an important factor affecting genome editing efficiency in porcine oocytes. *Theriogenology* 2018; **108**: 29–38. [Medline] [CrossRef]

29. **Zuo E, Cai Y-J, Li K, Wei Y, Wang B-A, Sun Y, Liu Z, Liu J, Hu X, Wei W, Huo X, Shi L, Tang C, Liang D, Wang Y, Nie YH, Zhang CC, Yao X, Wang X, Zhou C, Ying W, Wang Q, Chen RC, Shen Q, Xu GL, Li J, Sun Q, Xiong ZQ, Yang H.** One-step generation of complete gene knockout mice and monkeys by CRISPR/Cas9-mediated gene editing with multiple sgRNAs. *Cell Res* 2017; **27**: 933–945. [Medline] [CrossRef]

30. **Certo MT, Gwiazda KS, Kuhar R, Sather B, Curinga G, Mandt T, Brault M, Lambert AR, Baxter SK, Jacoby K, Ryu BY, Kiem HP, Gouble A, Paques F, Rawlings DJ, Scharenberg AM.** Coupling endonucleases with DNA end-processing enzymes to drive gene disruption. *Nat Methods* 2012; **9**: 973–975. [Medline] [CrossRef]

31. **Hu L, Kim TM, Son MY, Kim S-A, Holland CL, Tateishi S, Kim DH, Yew PR, Montagna C, Dumitrache LC, Hasty P.** Two replication fork maintenance pathways fuse inverted repeats to rearrange chromosomes. *Nature* 2013; **501**: 569–572. [Medline] [CrossRef]

32. **Mazur DJ, Perrino FW.** Excision of 3′ termini by the Trex1 and TREX2 3′-->5′ exonucleases. Characterization of the recombinant proteins. *J Biol Chem* 2001; **276**: 17022–17029. [Medline] [CrossRef]

33. **Brinkman EK, Chen T, Amendola M, van Steensel B.** Easy quantitative assessment of genome editing by sequence trace decomposition. *Nucleic Acids Res* 2014; **42**: e168–e168. [Medline] [CrossRef]

34. **Chang N, Sun C, Gao L, Zhu D, Xu X, Zhu X, Xiong J-W, Xi JJ.** Genome editing with RNA-guided Cas9 nuclease in zebrafish embryos. *Cell Res* 2013; **23**: 465–472. [Medline] [CrossRef]

35. **Hsu PD, Scott DA, Weinstein JA, Ran FA, Konermann S, Agarwala V, Li Y, Fine EJ, Wu X, Shalem O, Cradick TJ, Marraffini LA, Bao G, Zhang F.** DNA targeting specificity of RNA-guided Cas9 nucleases. *Nat Biotechnol* 2013; **31**: 827–832. [Medline] [CrossRef]

36. **Teixeira M, Py BF, Bosc C, Laubreton D, Moutin M-J, Marvel J, Flamant F, Markossian S.** Electroporation of mice zygotes with dual guide RNA/Cas9 complexes for simple and efficient cloning-free genome editing. *Sci Rep* 2018; **8**: 474. [Medline] [CrossRef]

37. **Allen F, Crepaldi L, Alsinet C, Strong AJ, Kleshchevnikov V, Angeli PD, Palenikova P, Kosicki M, Bassett AR, Harding H, et al.** Mutations generated by repair of Cas9-induced double strand breaks are predictable from surrounding sequence. *bioRxiv* 2018; 400341; doi: https://doi.org/10.1101/400341.

38. **Bothmer A, Phadke T, Barrera LA, Margulies CM, Lee CS, Buquicchio F, Moss S, Abdulkerim HS, Selleck W, Jayaram H, Myer VE, Cotta-Ramusino C.** Characterization of the interplay between DNA repair and CRISPR/Cas9-induced DNA lesions at an endogenous locus. *Nat Commun* 2017; **8**: 13905. [Medline] [CrossRef]

39. **Ayabe S, Nakashima K, Yoshiki A.** Off- and on-target effects of genome editing in mouse embryos. *J Reprod Dev* 2019; **65**: 1–5. [Medline] [CrossRef]

40. **Park K-E, Powell A, Sandmaier SES, Kim C-M, Mileham A, Donovan DM, Telugu BP.** Targeted gene knock-in by CRISPR/Cas ribonucleoproteins in porcine zygotes. *Sci Rep* 2017; **7**: 42458. [Medline] [CrossRef]

41. **Zhou X, Wang L, Du Y, Xie F, Li L, Liu Y, Liu C, Wang S, Zhang S, Huang X, Wang Y, Wei H.** Efficient generation of gene-modified pigs harboring precise orthologous human mutation via CRISPR/Cas9-induced homology-directed repair in zygotes. *Hum Mutat* 2016; **37**: 110–118. [Medline] [CrossRef]

42. **Nakade S, Mochida K, Kunii A, Nakamae K, Aida T, Tanaka K, Sakamoto N, Sakuma T, Yamamoto T.** Biased genome editing using the local accumulation of DSB repair molecules system. *Nat Commun* 2018; **9**: 3270. [Medline] [CrossRef]